

Abstract

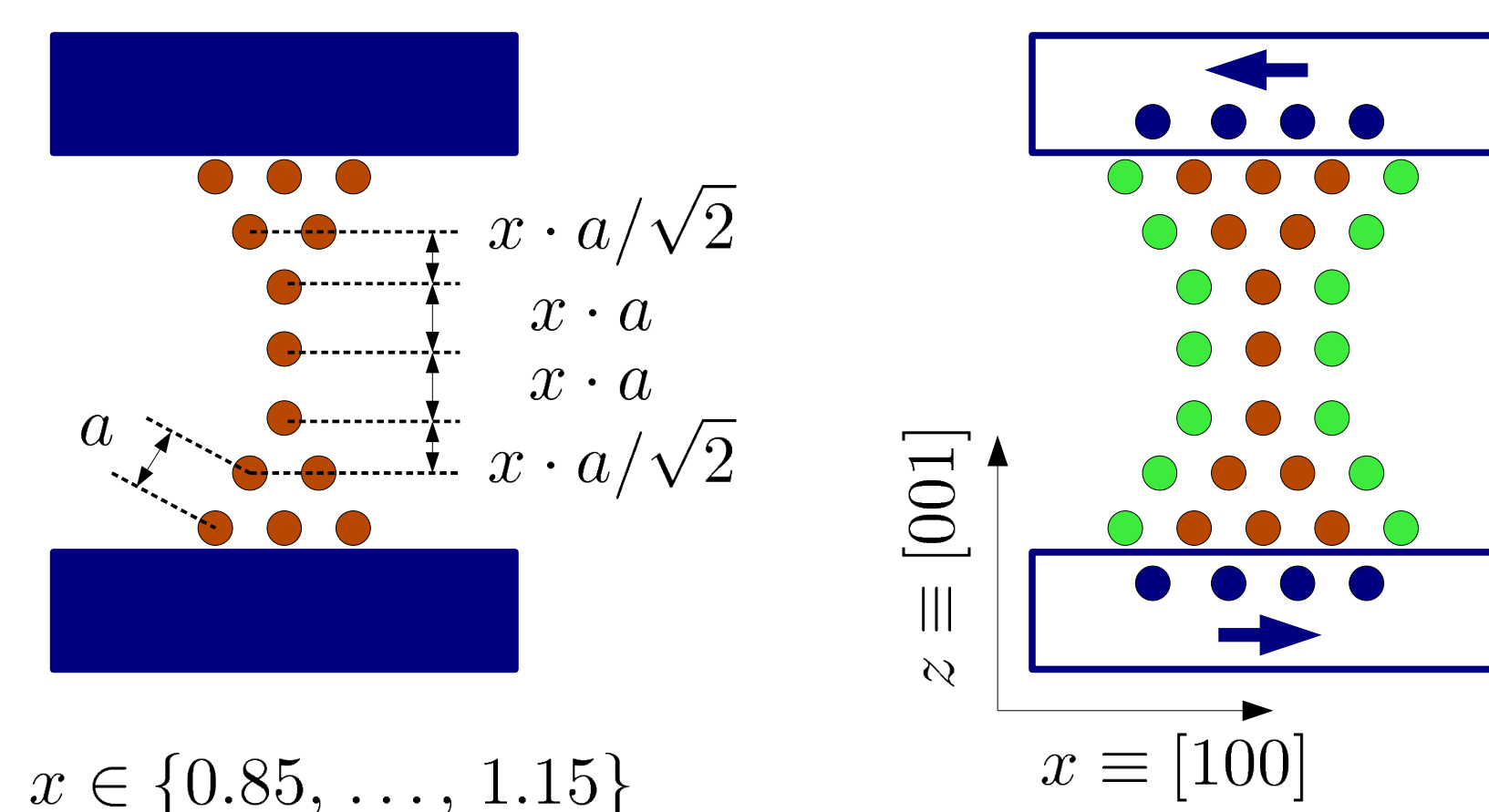
The recent technological development made it possible to build nano-sized structures which can play important role in wide range of applications. The theoretical studies exploring the quantum-effects of atomic-sized systems are of primary importance. In the present poster we investigate theoretically different properties of magnetic nanoparticles.

In order to model a break-junction a double pyramid cobalt nano-particle with a single cobalt atom between the tips of the pyramids has been chosen. The system was supported by two semi-infinite magnetically oppositely aligned Co substrate forming a domain wall through the contact.

To find the magnetic ground state configuration two methods have been used and compared: simple magnetic model (continuous, isotropic Heisenberg model) and a density functional theory based electronic structure calculation.

The magnetic configuration of the systems have been determined for various spatial separations of the substrates. We have found that the Neel type of domain wall is energetically more preferable than the Bloch wall for any length of the contact. The magnetic anisotropy energy of the central atom has been also analyzed. The anisotropy constants up to second order have been determined.

The physical system



The geometry of the contact viewed from the $[100]$ direction. On the left, we depict the supporters below and above the double pyramids as blue rectangles. The cobalt atoms forming the cobalt contact are represented by brown balls. a denotes the nearest neighbor distance between the atoms in the fcc structure. We tuned the length of the contact via x , picking up the values 0.85, 0.90, 0.95, 1.00, 1.05, 1.10 and 1.15 in this study. (Note: only the marked distances were changed, all the others were unchanged.)

On the right we present the embedded cluster. It consists of atoms from the supporters (blue balls), the cobalt nanocontact itself (brown balls) and the nearest neighbor shell around the contact (green balls). We indicate that the supporters are magnetized oppositely: $[100]$ and $[\bar{1}00]$ direction. (blue arrows)

Isotropic Heisenberg model

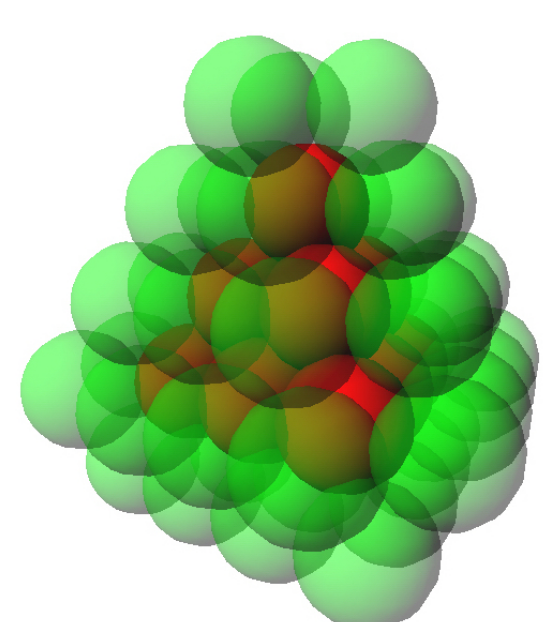
$$\mathcal{H} = \frac{1}{2} \sum_{i \neq j} J_{ij} \sigma_i \cdot \sigma_j$$

Invariant under global spin rotation. The boundary conditions are invariants under global spin rotation around the $[100]$ axis.

Configurations rotated around the $[100]$ axis are equivalent.

Embedded cluster Korringa–Kohn–Rostoker method

The electronic structure of the contact has been determined by means of the embedded cluster Green's function technique as combined with the KKR method.¹



$$\tau_C(\varepsilon) = (\mathbf{t}_C^{-1}(\varepsilon) - \mathbf{t}_h^{-1}(\varepsilon) + \tau_h^{-1}(\varepsilon))^{-1} \quad (1)$$

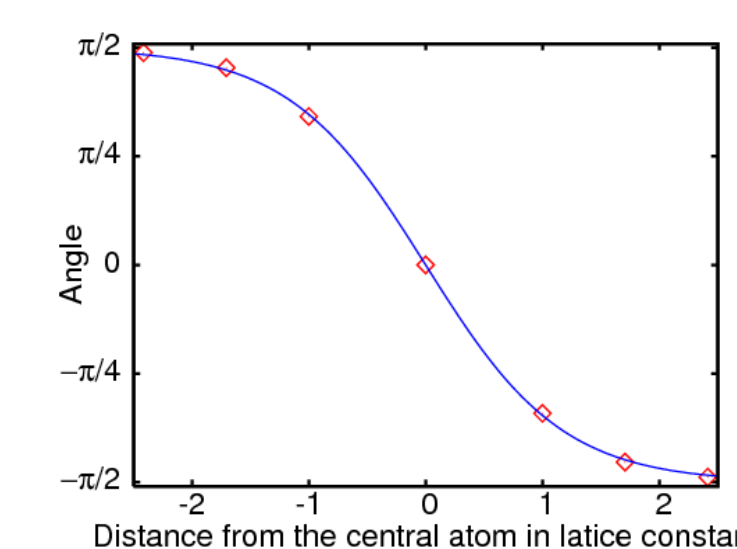
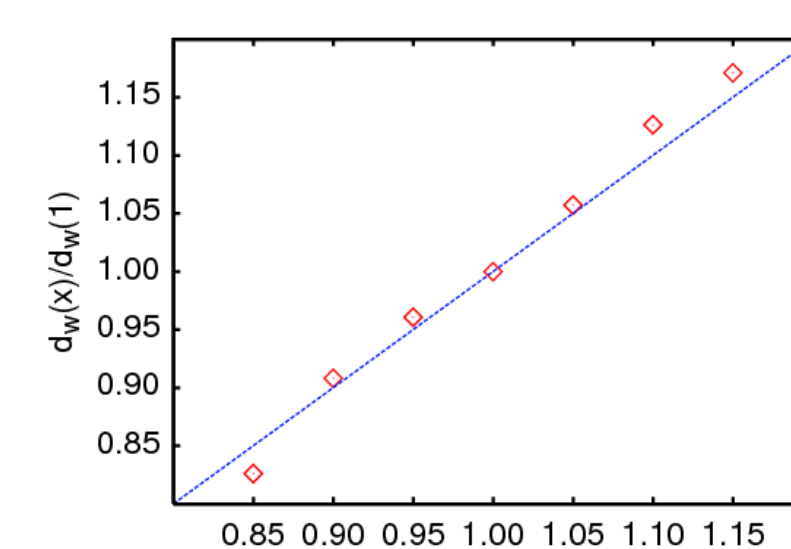
$$E_b = \int_{-\infty}^{E_F} (\varepsilon - E_F) n(\varepsilon) d\varepsilon = -\frac{1}{\pi} \text{Im} \int_{-\infty}^{E_F} \text{Tr} \ln \tau_C(\varepsilon) d\varepsilon \quad (2)$$

The essential quantity of the EC-KKR method, namely the scattering path operator (SPO), corresponding to a finite cluster C embedded into a host system can be obtained from the above equation, Eq. (1), where $\mathbf{t}_h(\varepsilon)$ and $\tau_h(\varepsilon)$ denote the single-site scattering matrix and the SPO matrix for the host confined to the sites in C , respectively, while \mathbf{t}_C denotes the single-site scattering matrices of the embedded atoms.

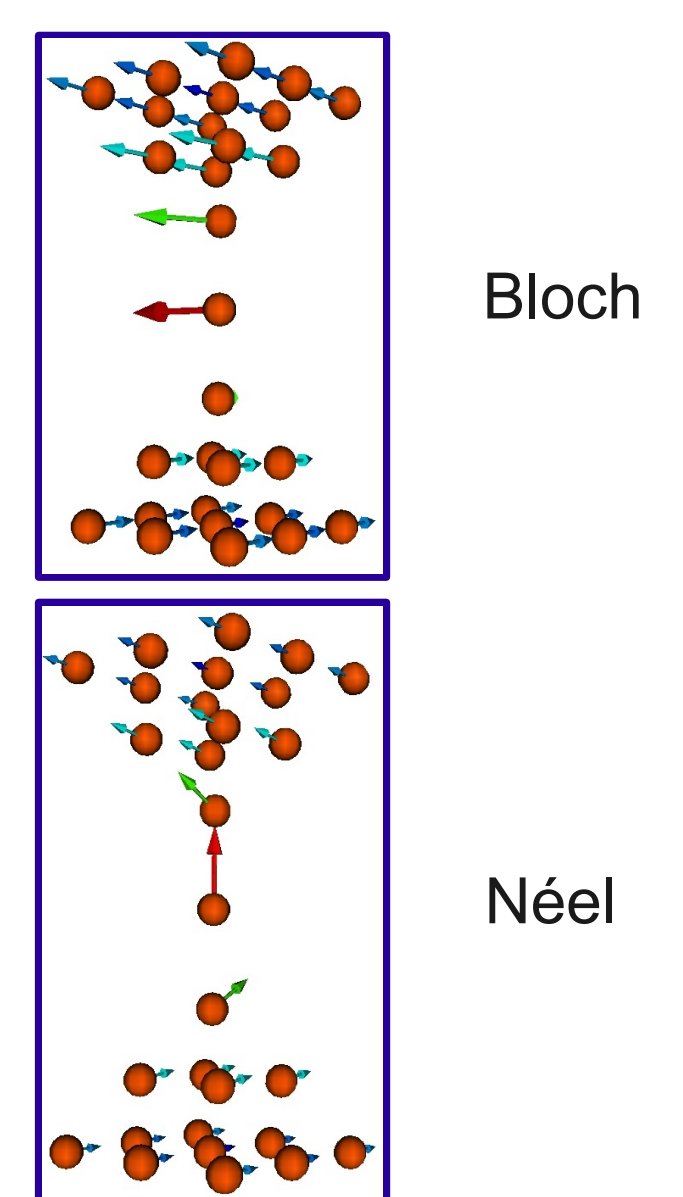
A newly developed Newton–Raphson iteration is based on the gradients of the band energy (see Eq. (2)) against the transverse change of the exchange field, where ε_F is the Fermi level and $n(\varepsilon)$ is the density of states.

Domain wall through the nano-contact

Naturally, a domain wall is formed through the nano-contact. The width of the domain wall can be determined by fitting a hyperbolic tangent function. For the clear interpretation the width of the walls is normalized to the width of the domain wall belonging to $x = 1$. The slope of the curve is almost the same as the slope of the identity demonstrating that the width of the domain wall follows the change of the lengths of the point contact. The results of our calculations confirm Bruno's conclusion in Ref. 3.

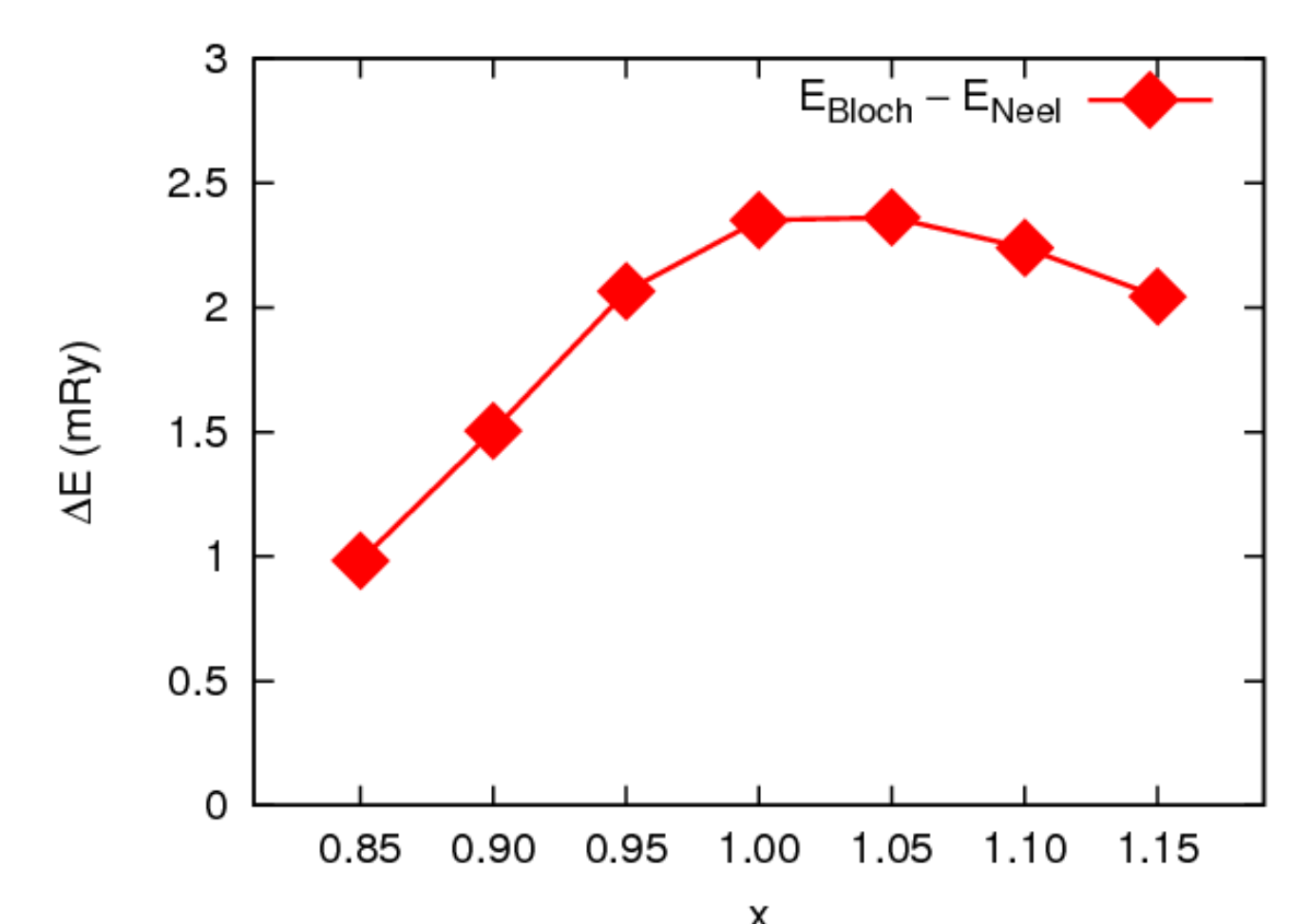
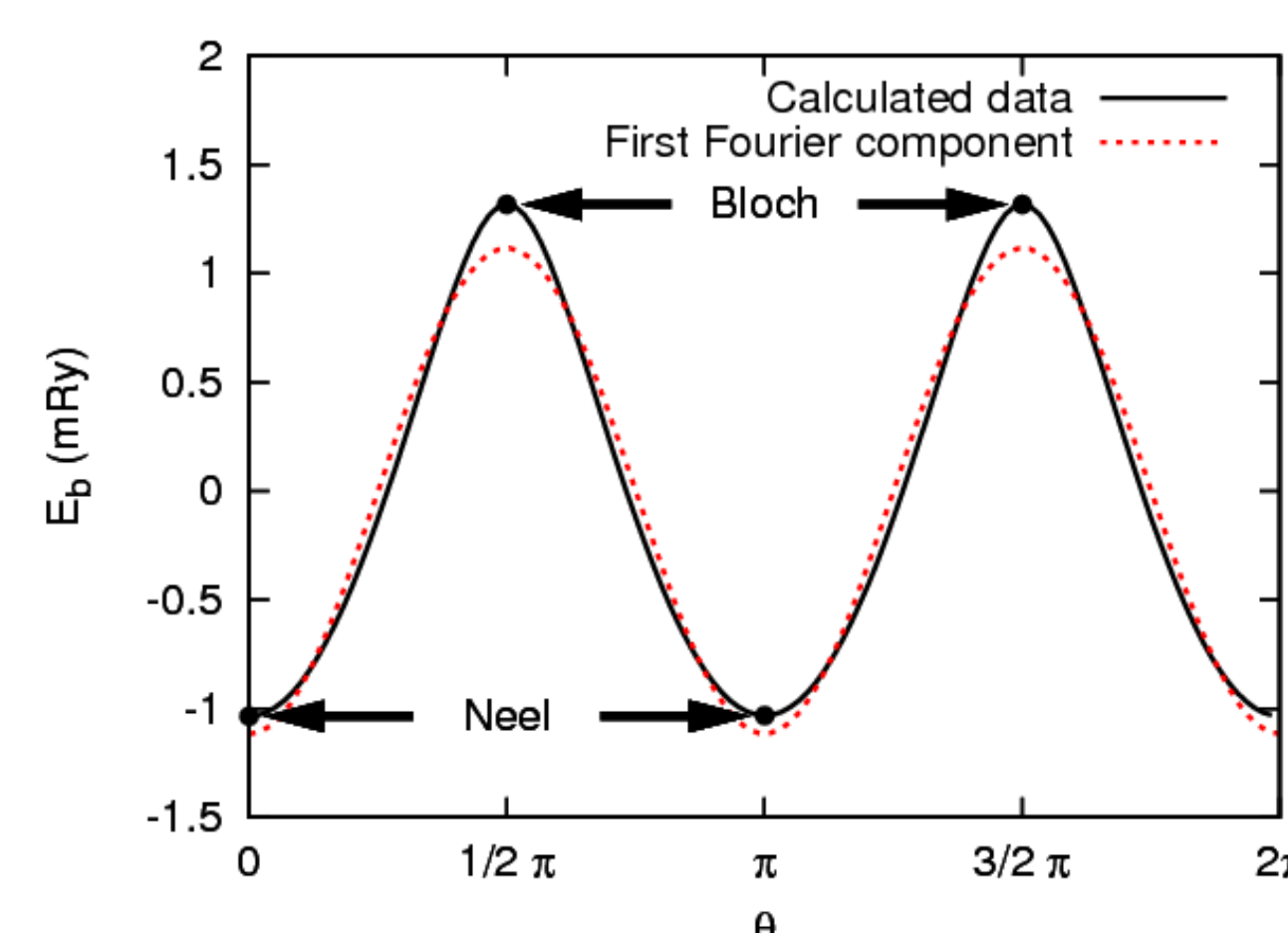


$$\varphi(z) = -\frac{\pi}{2} \text{th} \left(\frac{z}{2d_w} \right)$$



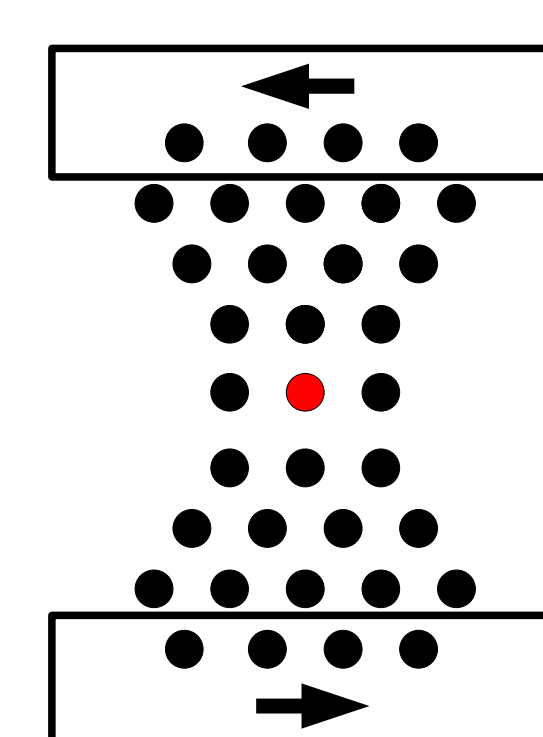
Global spin rotation around the $[100]$ axis

We investigated the anisotropy effects, which are originated from the spin–orbit coupling, by plotting the band energy of the system under a rotation around the $[100]$ axis. We expected an $E_b = a_1 \cos(2\theta)$ dependence on the polar angle coming from the uniaxial magnetic anisotropy. This investigation revealed that higher order components was also present in the anisotropy energy of the nano-contact.



Energy map of the central atom

Another investigation have been done in order to present the relevance of higher order terms beyond the simple Heisenberg model. All other spin directions were kept frozen into the ground state, while spin of the central atom was pointed into all directions. An energy map of the central atom was obtained and extracted in terms of the real spherical harmonics.



$$E_b(\dots, \vartheta, \varphi, \dots) = \sum_{l=0}^{\infty} \sum_{m=-l}^l E_{lm} Y_{lm}(\vartheta, \varphi)$$

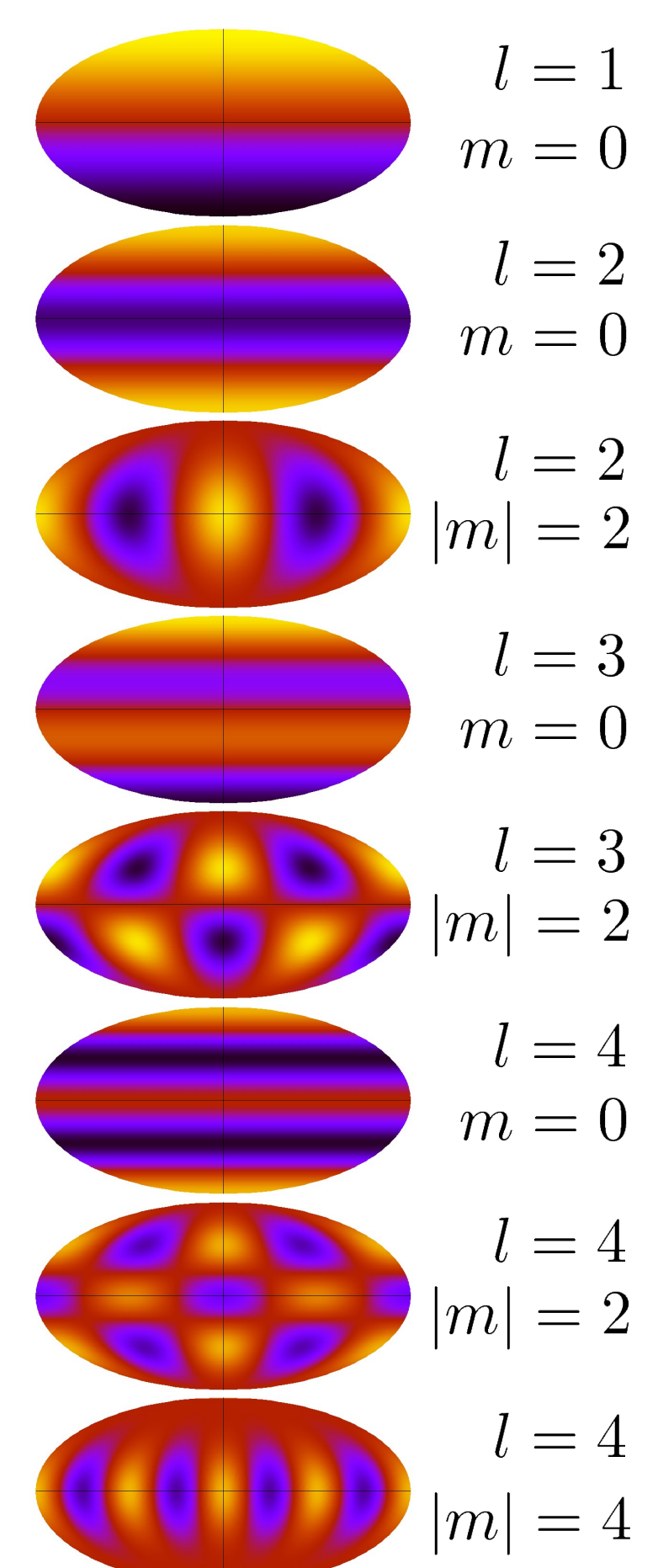


TABLE II. Expansion coefficients of the band energy of the central atom in the Néel wall according to real spherical harmonics. (Note: all other coefficients not listed here are zeros.) The unit is Rydberg.

l	$x=0.85$	$x=0.90$	$x=0.95$	$x=1.00$	$x=1.05$	$x=1.10$	$x=1.15$
1	$\frac{1}{2\sqrt{3}} \frac{z}{r}$	$-1.77 \cdot 10^{-2}$	$-1.81 \cdot 10^{-2}$	$-1.73 \cdot 10^{-2}$	$-1.56 \cdot 10^{-2}$	$-1.41 \cdot 10^{-2}$	$-1.29 \cdot 10^{-2}$
2	$\frac{1}{2\sqrt{5}} (3z^2 - 1)$	$-1.86 \cdot 10^{-3}$	$-2.21 \cdot 10^{-3}$	$-2.44 \cdot 10^{-3}$	$-2.38 \cdot 10^{-3}$	$-2.27 \cdot 10^{-3}$	$-2.09 \cdot 10^{-3}$
	$\frac{1}{2\sqrt{5}} (x^2 - y^2)$	$3.16 \cdot 10^{-4}$	$1.87 \cdot 10^{-4}$	$1.02 \cdot 10^{-4}$	$3.75 \cdot 10^{-5}$	$-2.13 \cdot 10^{-5}$	$-6.78 \cdot 10^{-5}$
3	$\frac{1}{2\sqrt{7}} (5z^3 - 3z)$	$3.03 \cdot 10^{-4}$	$2.25 \cdot 10^{-4}$	$1.20 \cdot 10^{-4}$	$5.22 \cdot 10^{-5}$	$-2.03 \cdot 10^{-5}$	$-1.05 \cdot 10^{-4}$
	$\frac{1}{2\sqrt{7}} (x^2 - y^2)z$	$-1.46 \cdot 10^{-5}$	$-6.82 \cdot 10^{-6}$	$3.17 \cdot 10^{-7}$	$7.91 \cdot 10^{-6}$	$1.44 \cdot 10^{-5}$	$1.96 \cdot 10^{-5}$
4	$\frac{3}{16} \sqrt{\frac{1}{5}} (35z^4 - 30z^2 + 3)$	$-4.60 \cdot 10^{-5}$	$1.26 \cdot 10^{-4}$	$3.38 \cdot 10^{-4}$	$3.63 \cdot 10^{-4}$	$3.71 \cdot 10^{-4}$	$3.57 \cdot 10^{-4}$
	$\frac{3}{8} \sqrt{\frac{2}{5}} (x^2 - y^2)(7z^2 - 1)$	$2.45 \cdot 10^{-6}$	$9.21 \cdot 10^{-6}$	$1.36 \cdot 10^{-5}$	$7.96 \cdot 10^{-6}$	$3.76 \cdot 10^{-6}$	$1.06 \cdot 10^{-7}$
	$\frac{3}{16} \sqrt{\frac{2}{5}} (x^4 - 6x^2y^2 + y^4)$	$-5.05 \cdot 10^{-7}$	$-3.87 \cdot 10^{-7}$	$-1.36 \cdot 10^{-6}$	$-2.98 \cdot 10^{-6}$	$-6.45 \cdot 10^{-6}$	$-1.38 \cdot 10^{-5}$

The higher order contributions can not be explained by only on-site anisotropy and pairwise exchange interactions.

References

- B. Lazarovits, L. Szunyogh, and P. Weinberger, Phys. Rev. B **65**, 104441 (2002).
- A. I. Liechtenstein, *et al.*, J. Mag. Mag. Materials **67**, 65 (1987).
- P. Bruno, Phys. Rev. Lett. **83**, 2425 (1999).

Acknowledgements

Financial support was provided by the Hungarian Research Foundation (Contracts No. OTKA K77771) and by the New Hungary Development Plan (Project No. TÁMOP-4.2.1/B-09/1/KMR-2010-0002).